

Type 1 Sodium-dependent Phosphate Transporter (SLC17A1 Protein) Is a Cl⁻-dependent Urate Exporter*^[S]

Received for publication, March 16, 2010, and in revised form, June 2, 2010. Published, JBC Papers in Press, June 21, 2010, DOI 10.1074/jbc.M110.122721

Masafumi Iharada[‡], Takaaki Miyaji[§], Takahiro Fujimoto[‡], Miki Hiasa[‡], Naohiko Anzai[¶], Hiroshi Omote[‡], and Yoshinori Moriyama^{‡§1}

From the [‡]Department of Membrane Biochemistry, Okayama University Graduate School of Medicine, Dentistry, and Pharmaceutical Sciences, and the [§]Advanced Science Research Center, Okayama University, Okayama 700-8530 and the [¶]Department of Pharmacology, Kyorin University School of Medicine, Tokyo 181-8611, Japan

SLC17A1 protein (NPT1) is the first identified member of the SLC17 phosphate transporter family and mediates the transmembrane cotransport of Na⁺/P_i in oocytes. Although this protein is believed to be a renal polyspecific anion exporter, its transport properties are not well characterized. Here, we show that proteoliposomes containing purified SLC17A1 transport various organic anions such as *p*-aminohippuric acid and acetylsalicylic acid (aspirin) in an inside positive membrane potential ($\Delta\psi$)-dependent manner. We found that NPT1 also transported urate. The uptake characteristics were similar to that of SLC17 members in its Cl⁻ dependence and inhibitor sensitivity. When arginine 138, an essential amino acid residue for members of the SLC17 family such as the vesicular glutamate transporter, was specifically mutated to alanine, the resulting mutant protein was inactive in $\Delta\psi$ -dependent anion transport. Heterologously expressed and purified human NPT1 carrying the single nucleotide polymorphism mutation that is associated with increased risk of gout in humans exhibited 32% lower urate transport activity compared with the wild type protein. These results strongly suggested that NPT1 is a Cl⁻-dependent polyspecific anion exporter involved in urate excretion under physiological conditions.

The kidney plays a principle role in the excretion of organic anions including metabolites and xenobiotics. This excretion occurs transcellularly across renal tubular epithelial cells via two distinct transport systems. On the basolateral membrane, the OAT1 (organic anion transporter 1) and the organic anion transporter 3 (OAT3) may actively take up *p*-aminohippuric acid (PAH),² a typical substrate of organic transport systems through exchange of intracellular dicarboxylates such as α -ke-

toglutarate (1–4). Organic anions are then excreted from the apical membrane into urine. Although this step is mediated through voltage-driven organic anion transporter(s), the molecular nature and the precise functional properties of this efflux system(s) is far less understood (1–4).

SLC17A1 protein (NPT1) is the first identified member of the SLC17 type 1 phosphate transporter family (5). NPT1 is expressed in the apical membrane of renal tubular cells and mediates Na⁺ and inorganic phosphate cotransport when expressed in oocytes (5–7). Oocytes expressing rabbit NPT1 also take up neutral red and benzylpenicillin (7). HEK293 cells expressing human NPT1 (hNPT1) take up various organic anions such as PAH (8). Oocytes expressing the pig SLC17A1 ortholog, OATv1, also exhibit electrogenic entry of PAH (9). Based on these observations, NPT1 is believed to be the voltage-driven organic anion transporter itself (8, 9). However, the direction of the transport of organic anions measured in these studies is opposite to that expected under physiological conditions, and the $\Delta\psi$ -driven uptake of organic anions by either NPT1 or OATv1 was not reported. Thus, it is still unclear whether NPT1 acts as a voltage-driven polyspecific anion exporter.

In addition to SLC17A1, eight other transporters belong to the SLC17 family (5, 10). SLC17A2, -A3, and -A4 are the orthologs of SLC17A1 (5). SLC17A5 protein is a biphasic transporter. When present in lysosomes, it acts as a H⁺/sialic acid cotransporter (sialin) and when present in synaptic vesicles, it acts as a vesicular excitatory amino acid transporter (VEAT) (11). Proteins encoded by SLC17A6, -A7, and -A8 are vesicular glutamate transporters (VGLUT), and SLC17A9 protein is a vesicular nucleotide transporter (VNUT) (5, 10). VGLUTs, VEAT, and VNUT all take up the respective anionic substrates in a $\Delta\psi$ -dependent manner. Furthermore, they all require Cl⁻ for the transport activities and are highly sensitive to DIDS and Evans blue. Arg¹⁸⁴ of VGLUT2, a charged amino acid residue in the transmembrane regions conserved in all members, which corresponds to Arg¹³⁸ of NPT1 (supplemental Fig. S1), is essential for their transport activity (5, 10–12). Hence, it is reasonable to assume that NPT1 also shares these properties and acts as a voltage-driven polyspecific anion exporter. Very recently, SNP in human SLC17A1 was found to be associated with the development of gout (13, 14, 15). Thus, it would be interesting

vesicular excitatory amino acid transporter; VGLUT, vesicular glutamate transporter; VNUT, vesicular nucleotide transporter; SCN, thiocyanate.

* This work was supported in part by grants-in-aid from the Japanese Ministry of Education, Science, Sports, and Culture (to H. O. and Y. M.), the Ajinomoto 3ARP, the Brain Science Foundation, and the Salt Science Foundation (to Y. M.).

[S] The on-line version of this article (available at <http://www.jbc.org>) contains supplemental "Experimental Procedures" and Figs. S1–S5.

¹ To whom correspondence should be addressed: Dept. of Membrane Biochemistry, Okayama University Graduate School of Medicine, Dentistry and Pharmaceutical Sciences, Okayama 700-8530, Japan. Tel.: 86-251-7933; Fax: 86-251-7933; E-mail: moriyama@pharm.okayama-u.ac.jp.

² The abbreviations used are: PAH, *p*-aminohippuric acid; $\Delta\psi$, membrane potential; hNPT1, human NPT1; VGLUT, vesicular glutamate transporters; DIDS, 4,4'-diisothiocyanostillbene-2,2'-disulfonic acid; MOPS, 3-morpholinopropane sulfonic acid; NPPB, 5-nitro-2-(3-phenylpropylamino) benzoic acid; VGAT, vesicular GABA transporter; DMSO, dimethyl sulfoxide; VEAT,

NPT1 Is a Cl⁻-dependent Urate Exporter

to determine whether urate is a substrate for NPT1 and if so, whether the SNP mutant exhibits decreased urate transport activity.

We have investigated these issues using proteoliposomes containing purified NPT1. Here, we show that NPT1 is a $\Delta\psi$ -driven, Cl⁻-dependent, and polyspecific anion transporter. Our quantitative studies show that NPT1 is a urate exporter and that the SNP mutant possesses a decreased urate transport activity.

EXPERIMENTAL PROCEDURES

cDNA—cDNA of mouse SLC17A1 (accession no. BC013445) was cloned by PCR. cDNA of human SLC17A1 (accession no. NM_005074.3) was a gift from Dr. Toshihisa Ishikawa (RIKEN, Japan).

Expression of NPT1—Recombinant baculoviruses containing wild type and mutant mouse NPT1 cDNA were constructed using the Bac-to-Bac baculovirus expression system (Invitrogen) according to the manufacturer's protocol. NPT1 cDNA was amplified by PCR using the primers 5'-CACCATGGAGAACAGTGCCTCCC-3' and 5'-CTTTATTTTGGTGTGCTGACACT-3' for mouse NPT1 or 5'-CACCATGCAAATGGATAACCGTTG-3' and 5'-TCAGAGACGTGTGTGTTGT-TTTTCTTTA-3' for hNPT1 and ligated into a pENTR/D-TOPO vector. hNPT1 cDNA was transferred from the pENTR/D-TOPO vector to a destination vector and named pDEST10-hNPT1. The resulting cloned hNPT1 gene also encoded an N-terminal His₆ tag. DH10Bac cells carrying bacmid DNA were transformed with pDEST10-hNPT1. Recombinant bacmid was isolated from DH10Bac cells and used for transfection of Sf9 insect cells to generate recombinant baculoviruses. Sf9 cells were used for expression of NPT1 protein. Sf9 cells (6 × 10⁶ cells/10 cm dish) were grown in complete Trichoplusia ni Medium-Formulation Hink (TNP-FH) medium (Invitrogen) supplemented with 10% fetal bovine serum, 0.25 μg/ml Fungizone, and 100 μg/ml penicillin-streptomycin at 27 °C. Sf9 cells were infected by recombinant baculoviruses at a multiplicity of infection of one and cultured a further 72 h. Afterward, the cells were harvested for membrane preparation.

Mutagenesis—The R138A mutation of mouse NPT1 was introduced into pDEST10-NPT1 by PCR. The sequence was confirmed by nucleotide sequencing. The following primers were used: R138A, 5'-GTGTGTGCTGCTACTGCAGGG-3' (forward) and 5'-AGGTATTATAGACCCTCGTTATAGG-3' (reverse). To generate the hNPT1 mutant, T269I, we performed site-directed mutagenesis using the QuikChange site-directed mutagenesis kit (Stratagene) according to the manufacturer's instructions. The mutagenic oligonucleotide primers for generation of T269I were 5'-GTCTGGGCTATTTCCACCGGCAGTTTACTTTTTTC-3' (forward) and 5'-GAAA-AAAGTAAAAGTCCGGTGGAAATAGCCCAGAC-3' (reverse).

Purification—Insect cells (2–3 × 10⁸ cells) were suspended in 20 ml of buffer consisting of 20 mM Tris-HCl (pH 8.0), 0.1 M sodium acetate, 10% glycerol, 0.5 mM dithiothreitol, 10 μg/ml pepstatin A, and 10 μg/ml leupeptin and disrupted by sonication with a TOMY UD-200 tip sonifier. Cell lysates were centrifuged at 700 × g for 10 min to remove debris, and the resultant supernatant was centrifuged at 160,000 × g for 1 h. The

pellet (membrane fraction) was suspended and solubilized in 6 ml of buffer containing 20 mM MOPS-Tris (pH 7.0), 10% glycerol, 2% octylglucoside, 10 μg/ml pepstatin A, and 10 μg/ml leupeptin at ~10 mg protein/ml. After centrifugation at 260,000 × g for 30 min, the supernatant was added to 1 ml of nickel-nitrilotriacetic acid Superflow resin (Qiagen) and incubated for 4 h at 4 °C. The resin was washed with 20 ml of 20 mM MOPS-Tris (pH 7.0), 5 mM imidazole, 20% glycerol, and 1% octylglucoside in a column. NPT1 was eluted from the resin with 3 ml of the same buffer containing 60 mM imidazole. The eluate containing purified NPT1 was stored at -80 °C, where it was stable without loss of activity for at least a few months. The purity of the purified NPT1 was >80% with yield of 70%.

Reconstitution—Reconstitution of purified recombinant NPT1 into liposomes was carried out by the freeze-thaw method described previously (12). In brief, 20 μg NPT1 was mixed with liposomes (0.5 mg lipid; see below), frozen at -80 °C, and left at this temperature for at least 10 min. The mixture was thawed quickly by holding the sample tube in the hands. After thawing, the mixture was diluted 30-fold with reconstitution buffer (20 mM MOPS-Tris (pH 7.0), 0.15 M sodium acetate, 5 mM magnesium acetate, and 0.5 mM dithiothreitol). Proteoliposomes were sedimented by centrifugation at 200,000 × g for 1 h at 4 °C and suspended in 0.2 ml of 20 mM MOPS-Tris (pH 7.0) containing 0.1 M potassium acetate and 5 mM magnesium acetate. The mixture was homogenized until clear and divided into small aliquots. Under the condition, ~50% NPT1 incorporated into liposomes exhibited right-side orientation as assessed with protease digestion as described previously (12). Yield of NPT1 from the membrane was ~70%.

Transport Assay—Proteoliposomes (0.4 μg protein/single assay) were suspended in 20 mM MOPS-Tris (pH 7.0), 5 mM magnesium acetate, 4 mM KCl, and 0.15 M sodium acetate and incubated for 3 min at 27 °C. Valinomycin as a solution in DMSO was added to give a final concentration of 2 μM, and the mixture was incubated for a further 2 min. The assay was initiated by addition of 100 μM *p*-[glycyl-2-³H] PAH (0.6 MBq/μmol), [8-¹⁴C]urate (0.05 MBq/μmol), carboxyl-¹⁴C-labeled aspirin (0.05 MBq/μmol) or 7-¹⁴C-labeled salicylate (0.05 MBq/μmol); 120 μl aliquots were taken at the times indicated and centrifuged through a Sephadex G-50 (fine) spin column at 760 × g for 2 min (16). Radioactivity in the eluate was measured by a liquid scintillation counter.

For Cl⁻ transport, the reaction mixture containing 20 mM MOPS-Tris (pH 7.0), 5 mM magnesium acetate, 10 mM PAH, 0.15 M potassium acetate, 2 μM valinomycin, and 10 mM radioactive ³⁶Cl⁻ (740 MBq/g, American Radiolabeled Chemicals Inc.) was preincubated for 3 min at 27 °C. Proteoliposomes containing NPT1 (0.5 μg protein per assay) were added to the mixture to initiate the reaction and incubated for a further 1 min. Aliquots (130 μl) were taken at the times indicated and centrifuged through a Sephadex G-50 (fine) spin column at 760 × g for 2 min. Radioactivity in the eluate was measured. Essentially the same protocol was used for Cl⁻ transport by vesicular GABA transporter (VGAT)-containing proteoliposomes, except that 10 mM GABA was included in the assay mixture.

Purification and Reconstitution of Other Transporters—VEAT, VGLUT2, VNUT, and VGAT were purified, reconsti-

tuted into proteoliposomes, and assayed according to the published procedures (10–12, 17).

Measurement of $\Delta\psi$ — $\Delta\psi$ were measured by radioisotope distribution (17). Proteoliposomes were incubated in the standard assay condition in the presence of 20 μM [¹⁴C]SCN⁻ for 3 min, and the internal concentration of [¹⁴C]SCN⁻ was quantified as described. Internal volume of proteoliposomes were determined by measuring of exclusive volume with [¹⁴C]mannitol. Then, $\Delta\psi$ was calculated following formula: $\Delta\psi = RT/F \times \ln\{[\text{internal SCN}^-]/[\text{external SCN}^-]\}$, where R is the gas constant, T is the absolute temperature, and F is the Faraday constant.

Miscellaneous Procedures—Polyacrylamide gel electrophoresis in the presence of SDS and Western blotting were performed as described (18). Protein concentration was assayed using bovine serum albumin as a standard (19).

Data Analysis—All numerical values are shown as the mean \pm S.D. ($n = 3$ –6). Statistical significance was determined by Student's t test.

RESULTS

NPT1 Is a $\Delta\psi$ -driven PAH Transporter—As the first step of the study, we established a simple assay for NPT1. Wild type mouse NPT1 was expressed in insect cells, solubilized, purified, and reconstituted into asolectin liposomes according to a procedure published previously (10–12, 17). The degree of purification in the reconstituted liposomes was confirmed by SDS-PAGE followed by staining with Coomassie Brilliant Blue (Fig. 1A). The proteoliposomes contained a polypeptide with 56 kDa as a major protein, which was confirmed by silver staining (supplemental Fig. S2).

The reconstituted proteoliposomes were trapped with Na⁺. Addition of valinomycin generated a K⁺ diffusion potential of ~ -90 mV (positive inside) across the liposome membrane as revealed by the distribution of radiolabeled SCN⁻ and facilitated PAH uptake (Fig. 1B). In the absence of valinomycin, $\Delta\psi$ did not form, and little uptake was observed (Fig. 1B). Control liposomes lacking SLC17A1 exhibited only background level uptake (Fig. 1B). The valinomycin-evoked PAH uptake exhibited dose-dependence with apparent K_m and V_{max} values of 1.1 mM and 90 nmoles/min/mg protein, respectively (Fig. 1C). Neither inside acidic pH gradient nor inside negative $\Delta\psi$ facilitated PAH uptake (Fig. 1D). Furthermore, we specifically mutated Arg¹³⁸ to alanine. The mutant NPT1 was heterologously expressed, purified, and reconstituted using the procedure of wild type protein (Fig. 1A). We found that the R138A mutant was devoid of $\Delta\psi$ -dependent PAH uptake activity (Fig. 1B). These results suggested that NPT1 acted as a $\Delta\psi$ -driven PAH transporter and that Arg¹³⁸ is important for PAH transport activity. These results also clearly indicated that cross-contaminating protein, if any, did not contribute to the PAH uptake.

NPT1 Is a Cl⁻-dependent Polyspecific Anion Transporter—Subsequently, we asked whether NPT1 shared transport properties with other SLC17 members. We found that NPT1-mediated $\Delta\psi$ -driven PAH uptake requires Cl⁻. In the absence of Cl⁻ in the assay mixture, essentially no transport activity was detected (Fig. 2A). Transport activity appeared at ~ 2 mM Cl⁻ increased with increasing Cl⁻ concentration and reached a pla-

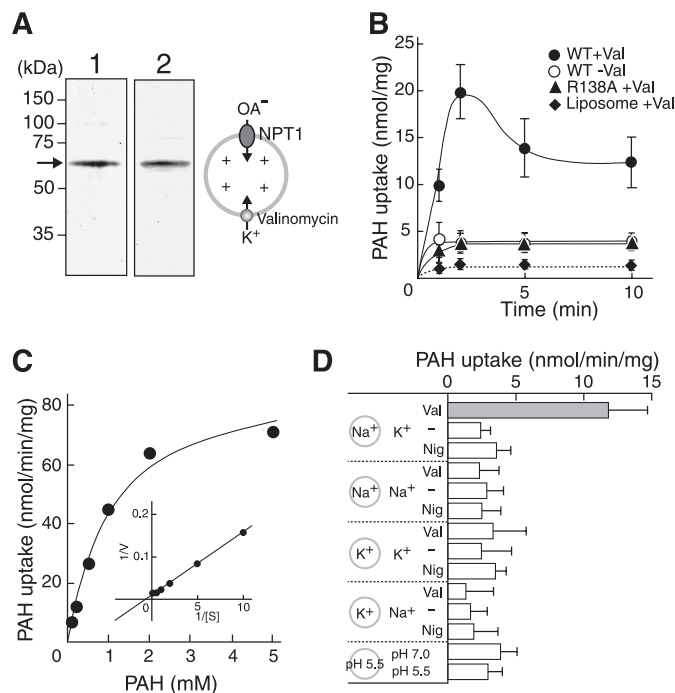


FIGURE 1. $\Delta\psi$ -driven PAH uptake by wild type and mutant NPT1. *A*, (left) purification and reconstitution of wild type and mutant NPT1 were performed as described under "Experimental Procedures." Purified and reconstituted proteins (10 μg) were electrophoresed on an 11% polyacrylamide gel and visualized by Coomassie Brilliant Blue staining. Lane 1, wild type; lane 2, R138A. The positions of molecular weight markers also are indicated. The position of NPT1 is marked by an arrow. Right, schema of *in vitro* assay of $\Delta\psi$ -dependent anion uptake. Upon the addition of valinomycin (Val), an inside positive $\Delta\psi$ was formed and facilitated the uptake of anions. *B*, time course of valinomycin-dependent PAH uptake by proteoliposomes containing wild type NPT1 (WT) (circles) and R138A (triangles). The reaction was started by adding radiolabeled PAH to a final concentration of 100 μM in the presence (closed symbols) or absence (open symbols) of valinomycin. For samples containing no valinomycin, an equivalent volume of solvent (DMSO) was added. *C*, dose-dependent PAH uptake by wild type NPT1 after 1 min was measured at the indicated concentrations. A Lineweaver-Burk plot is shown in the inset. *D*, energetics of PAH uptake by wild type NPT1. PAH uptake was measured under the ionic conditions as indicated. Nig, nigericin. Error bars represent mean \pm S.D. ($n = 3$ –5).

teau above 4 mM. Similar activation was observed by Br⁻ (Fig. 2B). I⁻ and F⁻ were slightly effective, whereas nitrate, sulfate, or thiocyanate were not (Fig. 2B). We then tested whether Cl⁻ protected DIDS-mediated inactivation because Cl⁻ competes with DIDS in VGLUT, suggesting the same binding site(s) for Cl⁻ and DIDS (12, 16, 17). We found that DIDS strongly inhibited $\Delta\psi$ -dependent PAH uptake with an ID₅₀ of 5 μM (Fig. 2C). Preincubation with 0.1 M Cl⁻ prevented DIDS-evoked inactivation (Fig. 2C). This effect was not observed when Cl⁻ was added after DIDS treatment (Fig. 2D).

The substrate specificity of NPT1 also was investigated. The *cis*-inhibitory profile indicated that PAH uptake was inhibited by acetylsalicylic acid (aspirin) and salicylate but not indomethacin, ibuprofen, diclofenac, etodolac, and mefenamic acid, suggesting that NPT1 recognized various anionic species as transport substrates (Table 1). Consistent with these observations, NPT1 transported aspirin with the K_m and V_{max} of 1.9 mM and 100 nmol/min/mg protein, respectively (Fig. 3, A and B). The R138A mutant did not transport aspirin (Fig. 3A). Similar to PAH uptake, Cl⁻ was required for activity, and DIDS inhibited the activity (Fig. 3, C and D). Similar uptake of radiolabeled salicylate was also observed (supplemental Fig. S3).

NPT1 Is a Cl⁻-dependent Urate Exporter

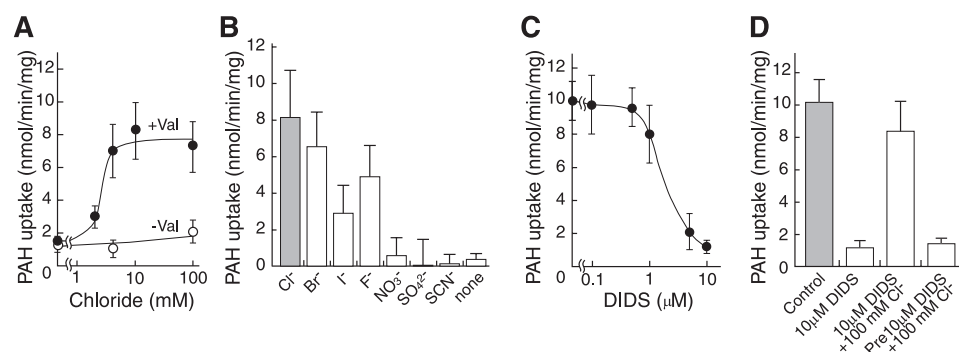


FIGURE 2. Cl⁻ dependence of $\Delta\psi$ -driven NPT1. *A*, Cl⁻ dependence on PAH uptake. The uptake was measured after 1 min in the presence of the indicated concentrations of Cl⁻. Part of the potassium acetate in the reaction mixture was replaced with the indicated concentration of KCl. *B*, anion selectivity. PAH uptake was measured in the presence of 4 mM indicated anions. *C*, the effect of DIDS on valinomycin (*Val*)-dependent PAH uptake. DIDS at the indicated concentrations was included in the assay medium. *D*, protection of PAH uptake by Cl⁻ against DIDS inactivation. Proteoliposomes were incubated in the buffer containing 4 or 100 mM Cl⁻ in the presence or absence of 10 μ M DIDS. After 1 min, valinomycin-evoked PAH uptake was measured. Error bars represent mean \pm S.D. ($n = 3-6$).

TABLE 1
Comparison of *cis* inhibition of PAH transport by NPT1

NPT1-mediated $\Delta\psi$ -dependent uptake of PAH was measured, and the effects of various compounds were examined as described in the legend to Fig. 1. Control activities (100%) correspond to 11.83 nmol/min/mg protein. Errors represent mean \pm S.D. ($n = 3-6$).

Compound (1 mM)	PAH uptake % of control
Control	100.0 \pm 9.5
Salicylate	33.2 \pm 9.1
Aspirin	46.0 \pm 13.8
Acetaminophen	60.3 \pm 12.5
Indomethacin	96.7 \pm 6.9
Ibuprofen	92.1 \pm 10.3
Diclofenac	90.9 \pm 9.5
Etodolac	91.3 \pm 11.2
Mefenamic acid	85.9 \pm 10.9
Uric acid	8.8 \pm 8.4

These results demonstrated that NPT1 was a polyspecific anion transporter with substrate specificity distinct from those of other SLC17 members. NPT1 did not transport D,L-glutamate, D,L-aspartate and ATP, which are substrates for other SLC17 family members (Table 2), and vice versa, the other SLC17 members did not transport PAH (Table 3).

Independence of Na⁺/P_i Cotransport and Anion Conductance—Because NPT1 possessed two other transport activities, *i.e.* the cotransport of Na⁺/P_i and anion conductance (6, 7, 16), it was important to discriminate mechanistic differences and/or similarities between the two activities and the $\Delta\psi$ -driven anion transport activity. When a Na⁺ gradient was imposed across the liposomal membranes, significant uptake of P_i was observed with a K_m of 6.3 mM and a V_{max} of 134 nmol/min/mg protein, indicating that NPT1 was actually a Na⁺/P_i cotransporter (supplemental Fig. S4, A and B). The Na⁺/P_i cotransporter did not require Cl⁻ (supplemental Fig. S4C). The R138A mutant possessed Na⁺/P_i cotransport activity comparable to that of the wild type protein. DIDS did not affect Na⁺/P_i cotransport (supplemental Fig. S4D). These properties are completely different from those of $\Delta\psi$ -dependent anion transport (Figs. 2 and 3).

When NPT1 is expressed in egg oocytes, an extraordinarily large anion conductance was observed (7, 16). Thus, it is interesting to ask the mechanistic differences and/or simi-

larities between $\Delta\psi$ -dependent anion transport and large anion conductance. It was reported that this anion conductance was relatively specific to Cl⁻ and highly sensitive to 5-nitro-2-(3-phenylpropylamino) benzoic acid (NPPB) and phenol red but not to DIDS (7). In contrast, we found that $\Delta\psi$ -dependent PAH transport was highly sensitive to DIDS, but less sensitive to NPPB and phenol red at equivalent concentrations (Fig. 4A). Moreover, in our system, no $\Delta\psi$ -dependent Cl⁻ movement was observed in the absence or presence of PAH, indicating that PAH transport was not accompanied by Cl⁻ movement

(Fig. 4B). Under similar assay conditions, VGAT that is known to cotransport 2 Cl⁻ and GABA (17), took up radiolabeled Cl⁻ in the presence of GABA (Fig. 4B) (17). Furthermore, only the background level of Cl⁻ uptake was observed by NPT1-containing proteoliposomes entrapped with PAH at 1 mM (data not shown). Taken together, these results suggested that Na⁺/P_i cotransport, anion conductance, and $\Delta\psi$ -dependent PAH transport shown here were not related to each other.

NPT1 Is a Urate Exporter—Finally, we attempted to identify the physiological substrate(s) of NPT1. Very recently, a SNP of NPT1 was identified that seemed to be related to elevated urate levels and risk of gout through genome-wide association studies (13). This suggested that NPT1 exports urate. We found that mouse NPT1 transported urate (Fig. 5A). Like other substrates, the R138A mutant was devoid of $\Delta\psi$ -dependent urate uptake activity (Fig. 5A). The K_m and V_{max} values were 1.1 mM and 149 nmol/min/mg protein, respectively (Fig. 5B). The $\Delta\psi$ -dependent urate uptake activity required Cl⁻ and was inhibited by low concentration of DIDS (Fig. 5, C and D). The *cis*-inhibitory profile indicated that PAH uptake was inhibited by cold urate (Table 1), and vice versa uptake of radiolabeled urate was inhibited by PAH, aspirin, and salicylate (Table 4). P_i at 1 mM slightly inhibited urate uptake (Table 4). These results suggested that urate shares the same recognition site(s) to those of other substrates.

Because urate is the end product of purine metabolism in humans, it is important to confirm urate transport activity in the human transporter. Therefore, we purified hNPT1 and its T269I SNP mutant associated with elevated urate levels and gout in humans (13) (Fig. 6A). Identity and similarity of amino acid sequences between hNPT1 and mouse NPT1 are 65.8 and 90.3%, respectively, indicating conserved nature of two proteins (supplemental Fig. S1). We found that proteoliposomes containing purified hNPT1 took up urate in a $\Delta\psi$ -mediated manner (Fig. 6, B and C). Furthermore, hNPT1 exhibited essentially the same transport characteristics with respect to kinetic parameters, substrate specificity, and requirement of Cl⁻ (Fig. 6, Table 4, and supplemental Fig. S5). Kinetic analysis indicated that proteoliposomes containing the same amount of T269I mutant proteins as wild type hNPT1 exhibited 46% lowered V_{max} value

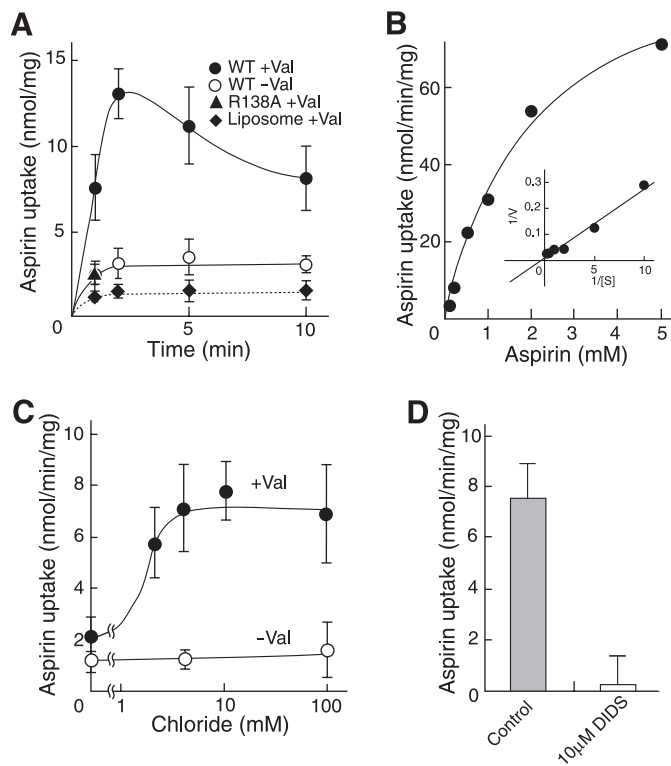


FIGURE 3. NPT1 is a polyspecific anion transporter. Uptake of aspirin was carried out as described in the legend to Fig. 1. *A–D*, NPT1 transports aspirin in a $\Delta\psi$ -dependent manner. Time course (*A*), dose dependence (*inset*) Lineweaver-Burk plot. (*B*), Cl⁻ dependence (*C*), and inhibition by DIDS at 10 μ M (*D*) are shown. Active transport by wild type (*WT*; circles) and R138A mutant (*triangle*) was initiated by the addition of either valinomycin (*Val*; closed symbols) or DMSO (control) (*open symbols*). Error bars represent mean \pm S.D. (*n* = 3–6).

TABLE 2

Uptake of substrates of other SLC17 members by NPT1

NPT1-mediated $\Delta\psi$ -dependent uptake of PAH, glutamate, aspartate, and ATP were measured as described in the legend to Fig. 1. Errors represent mean \pm S.D. (*n* = 3–6).

Substrate	Uptake
	<i>nmol/min/mg protein</i>
PAH	11.83 \pm 2.88
Glutamate	0.01 \pm 0.12
Aspartate	0.11 \pm 0.24
ATP	0.16 \pm 0.09

TABLE 3

Uptake of PAH by SLC17 members

Members of the SLC17 family were purified and reconstituted into liposomes. The $\Delta\psi$ -dependent uptake of 100 μ M PAH was measured as described in the legend to Fig. 1. The proteoliposomes showed the following transport activities for the authentic substrates: VEAT, $\Delta\psi$ -dependent aspartate uptake, 16.2 nmol/min/mg protein; VGLUT2, $\Delta\psi$ -dependent glutamate uptake, 8.2 nmol/min/mg protein; VNUT, $\Delta\psi$ -dependent ATP uptake, 8.0 nmol/min/mg protein. Errors represent mean \pm S.D. (*n* = 3–6).

Protein name	Gene name	PAH uptake
		<i>nmol/min/mg protein</i>
NPT1	SLC17A1	11.83 \pm 2.88
VEAT	SLC17A5	0.51 \pm 0.05
VGLUT2	SLC17A6	1.21 \pm 0.32
VNUT	SLC17A9	0.94 \pm 0.27

without affecting K_m value to those of wild type protein (Fig. 6, *B* and *C*). It is noteworthy that the T269I mutant also exhibited 41 and 38% decreased PAH and aspirin uptakes, respectively. These results indicated that hNPT1 is a urate exporter and

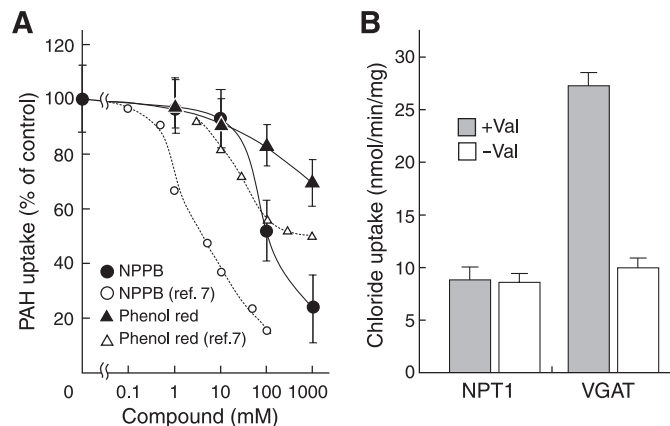


FIGURE 4. NPT1 is not a Cl⁻ transporter. *A*, NPPB and phenol red dose dependence on $\Delta\psi$ -dependent PAH uptake. The assay was performed in the presence or absence of either NPPB or phenol red at the indicated concentrations. The NPPB and phenol red dose dependence on anion conductance shown in Ref. 7 is also shown as a *dashed line* for comparison. *B*, absence of $\Delta\psi$ -dependent radioactive Cl⁻ uptake by NPT1-containing proteoliposomes. $\Delta\psi$ -dependent uptake of radioactive Cl⁻ by VGAT also is shown as a positive control. Error bars represent mean \pm S.D. (*n* = 3–5). *Val*, valinomycin.

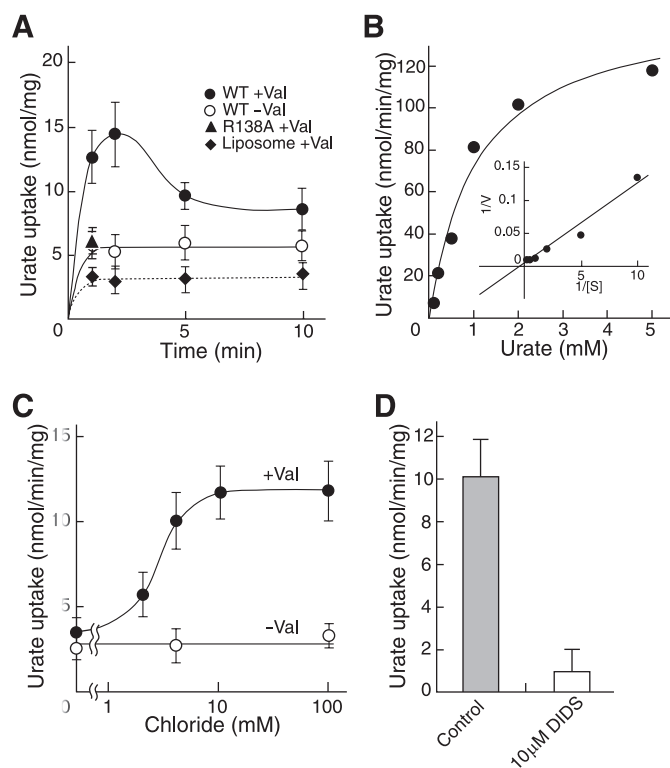


FIGURE 5. NPT1 is a urate exporter. Uptake of urate was carried out as described in the legend to Fig. 1. *A–D*, NPT1 transports urate in a $\Delta\psi$ -dependent manner. Time course (*A*), dose dependence (*inset*) Lineweaver-Burk plot. (*B*), Cl⁻ dependence (*C*), and inhibition by DIDS at 10 μ M (*D*) are shown. Active transport was initiated by the addition of either valinomycin (*Val*; closed symbols) or DMSO (control; open symbols). Error bars represent mean \pm S.D. (*n* = 3–5). *WT*, wild type.

hNPT1 possessing the T269I mutation may exhibit decreased urate excretion.

DISCUSSION

Since it was first identified, the transport properties of NPT1 and its orthologs have been characterized using transporter-expressing cultured cells or oocytes. However, an attempt to

NPT1 Is a Cl⁻-dependent Urate Exporter

elucidate the property as $\Delta\psi$ -driven anion exporter was unsuccessful. Here, we used a simple assay system containing purified NPT1 as the only protein and presented compelling evidence that NPT1 acts as a $\Delta\psi$ -dependent polyspecific anion exporter. The data are consistent with those of the physiologically identified anion transporter (1–4). We showed that NPT1 shared transport properties with VGLUTs, VEAT, and VNUT, anion transporting vesicular neurotransmitter transporters, with respect to driving force, anion requirement, and inhibitor sensitivities.

We elucidated three significant characteristics of the NPT1 phenotype. First, we presented direct evidence that NPT1 transports aspirin and salicylate. Although it is known that these compounds are excreted into the kidney, the transporter responsible for their renal excretion remains unclear. Recently, the tetracycline transporter-like protein (TETRAN) was shown to transport indomethacin (20). *Cis*-inhibition studies suggest that etodolac and mefenamic acid are also recognized by TETRAN, but not aspirin and salicylate (20). Thus, it is likely that NPT1 complements the transport activity of TETRAN, and that both transporters are involved in the renal excretion of nonsteroidal anti-inflammatory drugs.

The second important finding is that there is no direct relationship between $\Delta\psi$ -dependent polyspecific anion transport and anion conductance through NPT1. This issue is of particular significance because this is profoundly related to the

unsolved issue of how Cl⁻ activates VGLUTs, which are essential for glutamatergic neurotransmission. Two groups (including this study) have suggested that Cl⁻ stimulates VGLUTs upon binding (12, 21, 22), whereas Takamori and colleagues (23) have proposed recently that VGLUT1 is responsible for Cl⁻ permeability across the synaptic vesicle membranes through either glutamate/Cl⁻ cotransport or glutamate/Cl⁻ antiport. Here, we showed that NPT1 did not transport Cl⁻ even in the presence of extravesicular or intravesicular PAH, suggesting that Cl⁻ acts as an allosteric activator of NPT1, and hence, NPT1 is not a Cl⁻ transporter. Taking mechanistic similarity of NPT1 and VGLUTs, it is probable that Cl⁻ modulates VGLUTs upon binding (12, 21, 22). At present, we cannot explain the relationship between Cl⁻ dependence and large Cl⁻ conductance upon expression of NPT1 in oocytes. One of the plausible explanations is that the large Cl⁻ conductance is due to the interaction of NPT1 with oocyte proteins. Further studies will be necessary to clarify the issue.

The most important finding in the present study is that NPT1 is a urate transporter. Urate is an end product of purine metabolism in humans and acts a natural antioxidant with neuroprotective properties (24). In addition, Watanabe *et al.* (25) hypothesized that elevated serum urate levels caused by the loss of urate oxidase activity provided a survival advantage because hyperuricemia helped to maintain blood pressure levels under the low salt dietary conditions that prevailed in the middle to late Miocene period. Despite its beneficial role, the elevated serum urate level is associated with several metabolic disorders such as gout and kidney stones in humans (26). It is known that urate is excreted from renal proximal tubules by at least two distinct transporters, one of which is ABCG2, an ATP-driven ABC-type transporter (27). The second is an unidentified $\Delta\psi$ -driven anion transporter (28). The present results clearly indicated that NPT1 corresponded, at least in part, to this unidentified transporter. Decreased transport activities in both proteins are expected to lead to elevated blood urate levels and hence, to increased probability of gout. Consistent with this line of thought, it is known that SNPs associated with decreased activities of ABCG2 also are risk factors for gout (27, 28). We demonstrated here that the case is the same with NPT1; one SNP associated with gout also was linked to decreased urate transport activity.

Collectively, these results support the idea that NPT1 is involved in urate elimination from the body under physiological conditions, and its impairment is linked with occurrence of gout.

In conclusion, we presented evidence that NPT1 is a polyspecific anion exporter that participates in the renal excretion of urate and nonsteroidal anti-inflammatory drugs. Our simple assay is an efficient and highly sensitive procedure to evaluate transport activities of wild type and mutant transporters identified through genome-wide association studies.

TABLE 4

Comparison of *cis* inhibition of urate transport by hNPT1

hNPT1-mediated $\Delta\psi$ -dependent uptake of urate was measured, and the effects of various compounds were examined as described in the legend to Fig. 6. Control activities (100%) correspond to 11.82 nmol/min/mg protein. Phosphate was added as KPi. Similar inhibition was also given by NaPi. Errors represent mean \pm S.D. ($n = 3-6$).

Compound (1 mM)	Urate uptake % of control
Control	100.0 \pm 8.8
PAH	0.0 \pm 6.6
Salicylate	0.0 \pm 8.9
Aspirin	0.5 \pm 7.8
Diclofenac	78.9 \pm 14.9
Phosphate	69.6 \pm 8.6

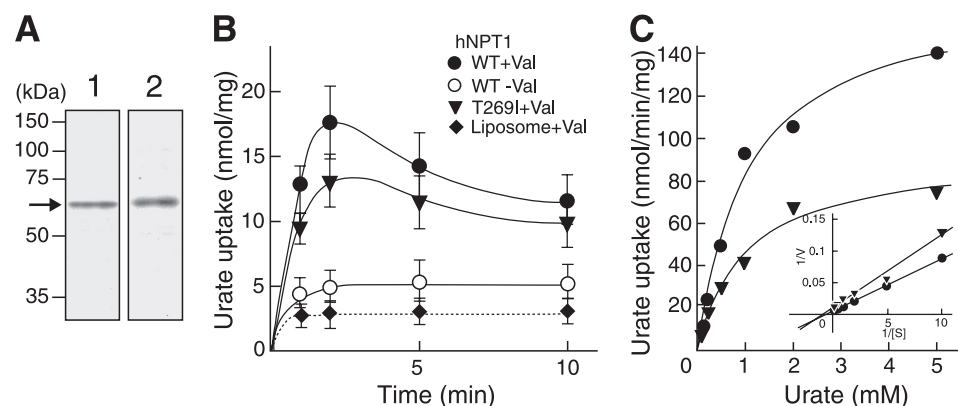


FIGURE 6. The effect of SNP on urate transport activity. Purification of human NPT1 and uptake of urate were carried out as described in the legend to Fig. 1. *A*, purified and reconstituted human NPT1 proteins (10 μ g) visualized by Coomassie Brilliant Blue staining. Lane 1, wild type (WT); lane 2, T269I. *B-C*, $\Delta\psi$ -dependent urate transport. Time course (*B*) and dose dependence (*inset*) Lineweaver-Burk plot. (*C*) are shown. Active transport by wild type (WT; circles) and T269I mutant (triangles) were initiated by the addition of either valinomycin (Val; closed symbols) or DMSO (control) (open symbols). Error bars represent mean \pm S.D. ($n = 3-5$).

Acknowledgments—We thank Dr. N. Juge for measurement of $\Delta\psi$, Dr. P. Jutabha and K. Fujiwara for preparation of cDNAs, and Drs. K. Higaki, F. Takayama, and T. Aiba for valuable discussions.

REFERENCES

- Pritchard, J. B., and Miller, D. S. (1993) *Physiol. Rev.* **73**, 765–796
- Inui, K. I., Masuda, S., and Saito, H. (2000) *Kidney. Int.* **58**, 944–958
- Koepsell, H. (2004) *Trends Pharmacol. Sci.* **25**, 375–381
- Wright, S. H., and Dantzer, W. H. (2004) *Physiol. Rev.* **84**, 987–1049
- Reimer, R. J., and Edwards, R. H. (2004) *Pflugers Arch.* **447**, 629–635
- Werner, A., Moore, M. L., Mantel, N., Biber, J., Semenza, G., and Murer, H. (1991) *Proc. Natl. Acad. Sci. U.S.A.* **88**, 9608–9612
- Busch, A. E., Schuster, A., Waldegger, S., Wagner, C. A., Zempel, G., Broer, S., Biber, J., Murer, H., and Lang, F. (1996) *Proc. Natl. Acad. Sci. U.S.A.* **93**, 5347–5351
- Uchino, H., Tamai, I., Yamashita, K., Minemoto, Y., Sai, Y., Yabuuchi, H., Miyamoto, K., Takeda, E., and Tsuji, A. (2000) *Biochem. Biophys. Res. Commun.* **270**, 254–259
- Jutabha, P., Kanai, Y., Hosoyamada, M., Chairoungdua, A., Kim, D. K., Iribe, Y., Babu, E., Kim, J. Y., Anzai, N., Chatsudthipong, V., and Endou, H. (2003) *J. Biol. Chem.* **278**, 27930–27938
- Sawada, K., Echigo, N., Juge, N., Miyaji, T., Otsuka, M., Omote, H., Yamamoto, A., and Moriyama, Y. (2008) *Proc. Natl. Acad. Sci. U.S.A.* **105**, 5683–5686
- Miyaji, T., Echigo, N., Hiasa, M., Senoh, S., Omote, H., and Moriyama, Y. (2008) *Proc. Natl. Acad. Sci. U.S.A.* **105**, 11720–11724
- Juge, N., Yoshida, Y., Yatsushiro, S., Omote, H., and Moriyama, Y. (2006) *J. Biol. Chem.* **281**, 39499–39506
- Urano, W., Taniguchi, A., Anzai, N., Inoue, E., Kanai, Y., Yamanaka, M., Endou, H., Kamatani, N., and Yamanaka, H. (2010) *Ann. Rheum. Dis.* **69**, 1232–1234
- Dehghan, A., Köttgen, A., Yang, Q., Hwang, S. J., Kao, W. L., Rivadeneira, F., Boerwinkle, E., Levy, D., Hofman, A., Astor, B. C., Benjamin, E. J., van Duijn, C. M., Witteman, J. C., Coresh, J., and Fox, C. S. (2008) *Lancet* **372**, 1953–1961
- Kolz, M., Johnson, T., Sanna, S., Teumer, A., Vitart, V., Perola, M., Mangino, M., Albrecht, E., Wallace, C., Farrall, M., Johansson, A., Nyholt, D. R., Aulchenko, Y., Beckmann, J. S., Bergmann, S., Bochud, M., Brown, M., Campbell, H., Connell, J., Dominiczak, A., Homuth, G., Lamina, C., McCarthy, M. I., Meitinger, T., Mooser, V., Munroe, P., Nauck, M., Peden, J., Prokisch, H., Salo, P., Salomaa, V., Samani, N. J., Schlessinger, D., Uda, M., Völker, U., Waeber, G., Waterworth, D., Wang-Sattler, R., Wright, A. F., Adamski, J., Whitfield, J. B., Gyllenstein, U., Wilson, J. F., Rudan, I., Pramstaller, P., Watkins, H., Doering, A., Wichmann, H. E., Spector, T. D., Peltonen, L., Völzke, H., Nagaraja, R., Vollenweider, P., Caulfield, M., Illig, T., and Gieger, C. (2009) *PLoS Genet.* **5**, e1000504
- Bröer, S., Schuster, A., Wagner, C. A., Bröer, A., Forster, I., Biber, J., Murer, H., Werner, A., Lang, F., and Busch, A. E. (1998) *J. Membr. Biol.* **164**, 71–77
- Juge, N., Muroyama, A., Hiasa, M., Omote, H., and Moriyama, Y. (2009) *J. Biol. Chem.* **284**, 35073–35078
- Moriyama, Y., Iwamoto, A., Hanada, H., Maeda, M., and Futai, M. (1991) *J. Biol. Chem.* **266**, 22141–22146
- Schaffner, W., and Weissmann, C. (1973) *Anal. Biochem.* **56**, 502–514
- Ushijima, H., Hiasa, M., Namba, T., Hwang, H. J., Hoshino, T., Mima, S., Tsuchiya, T., Moriyama, Y., and Mizushima, T. (2008) *Biochem. Biophys. Res. Commun.* **374**, 325–330
- Hartinger, J., and Jahn, R. (1993) *J. Biol. Chem.* **268**, 23122–23127
- Moriyama, Y., and Yamamoto, A. (1995) *J. Biol. Chem.* **270**, 22314–22320
- Schenck, S., Wojcik, S. M., Brose, N., and Takamori, S. (2009) *Nat. Neurosci.* **12**, 156–162
- Kutzing, M. K., and Firestein, B. L. (2008) *J. Pharmacol. Exp. Ther.* **324**, 1–7
- Watanabe, S., Kang, D. H., Feng, L., Nakagawa, T., Kanellis, J., Lan, H., Mazzali, M., and Johnson, R. J. (2002) *Hypertension* **40**, 355–360
- Becker, M. A., and Jolly, M. (2006) *Rheum. Dis. Clin. N. Am.* **32**, 275–293
- Woodward, O. M., Köttgen, A., Coresh, J., Boerwinkle, E., Guggino, W. B., and Köttgen, M. (2009) *Proc. Natl. Acad. Sci. U.S.A.* **106**, 10338–10342
- Hediger, M. A., Johnson, R. J., Miyazaki, H., and Endou, H. (2005) *Physiology* **20**, 125–133